

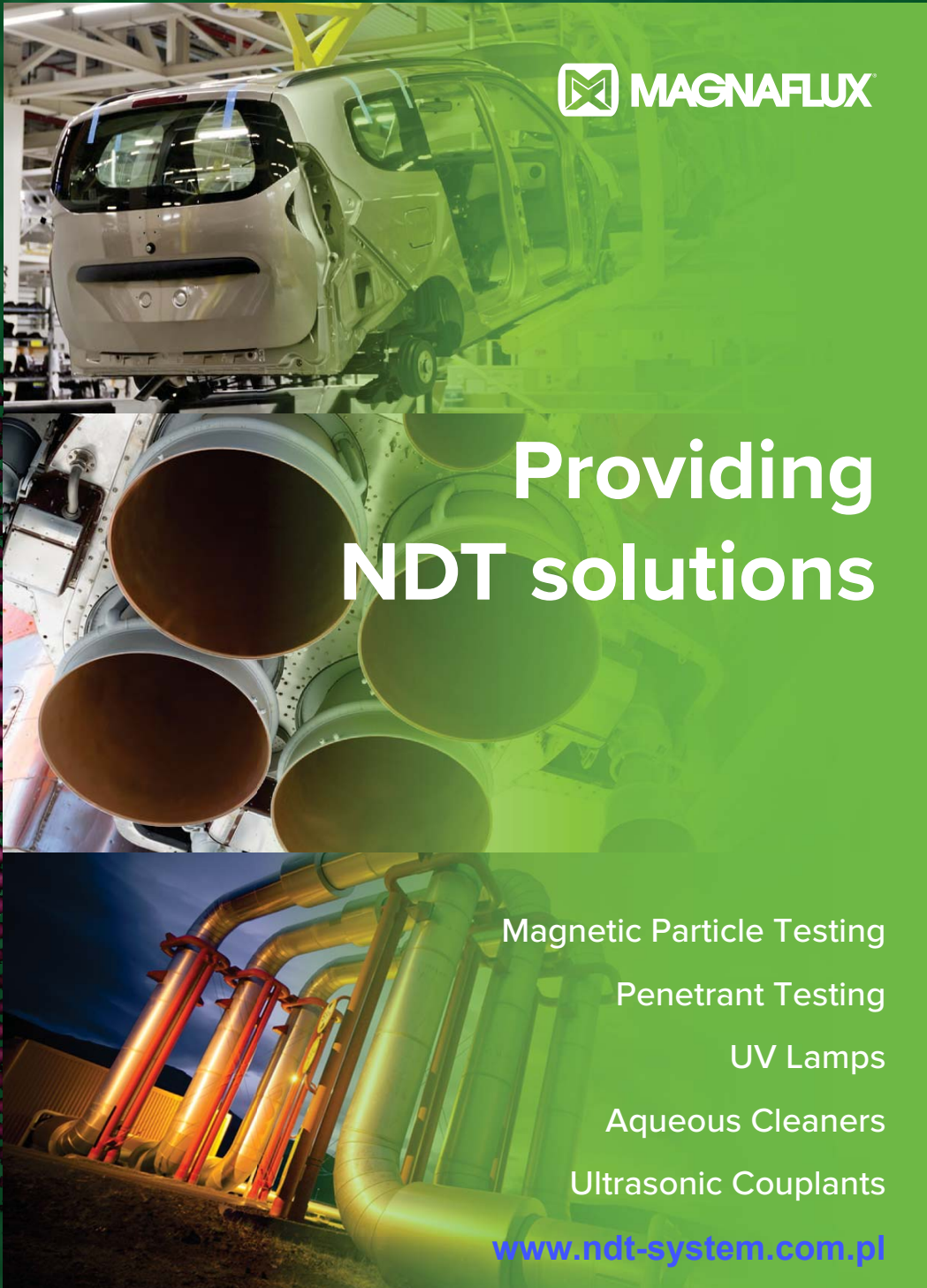
Badania Nieniszczące 1 - 4 / 2023 i Diagnostyka


Kwartalnik Naukowo-Techniczny

Nondestructive Testing and Diagnostics

50. KKBN

www.kkbn.pl



 **MAGNAFLUX**

Providing NDT solutions

- Magnetic Particle Testing
- Penetrant Testing
- UV Lamps
- Aqueous Cleaners
- Ultrasonic Couplants

www.ndt-system.com.pl

DXR75P-HR

Mały system obrazowania o najwyższej rozdzielczości do krytycznych zastosowań

Detektor DXR75P-HR daje wysoką rozdzielczość pikseli 75 μm , wymaganą do rozróżnienia drobnych szczegółów w krytycznych zastosowaniach. Detektor obejmuje kontrolę spoin klasy B według ISO 17636-2, dając precyzyjne obrazy spełniające najostrejsze wymagania.



Dzięki małej szerokości detektor jest idealny do tworzenia obrazów w sytuacjach o ograniczonej swobodzie ustawienia.

DXR75P-HR jest odpowiedni do zastosowań krytycznych, takich jak (ale bez ograniczenia):

- **kontrola spoin w przemyśle naftowym i gazowym oraz w energetyce i lotnictwie:**
 - rurociągi transportowe
 - złożone konstrukcje (odcinki rurociągu)
 - rury kotłowe
 - przewody paliwowe
 - rury ciśnieniowe
 - zbiorniki ciśnieniowe i magazynowe
- **kontrola spoin w okrętownictwie**

DXR140P-HE

Duży system obrazowania o wysokim kontraście do radiografii o wysokiej energii

DXR140P-HE jest idealnym przenośnym detektorem przeznaczonym do zastosowań o wysokiej energii (izotopowych). Optymalne wewnętrzne ekranowanie zapobiega promieniowaniu rozproszonemu o niskiej energii, ujemnie wpływającemu na jakość obrazu i żywotność elektroniki.



Detektor DXR140P-HE może być stosowany z izotopami i promieniowaniem RTG o wysokiej energii (powyżej 450 kV), jest odpowiedni do ogólnych zastosowań radiograficznych, takich jak (ale bez ograniczenia):

- **kontrola eksploatacyjna w przemyśle naftowym i gazowym oraz w energetyce:**
 - badanie korozji pod izolacją
 - pozycjonowanie zaworów
 - pomiar grubości ścianki
 - badanie podpór rurociągów
 - rury kotłowe
- **kontrola odlewów**
- **konserwacja, naprawa i przeglądy w lotnictwie**
- **przemysł zbrojeniowy i bezpieczeństwo**
- **kontrola konstrukcji:**
 - beton, mosty, podpory, ...
- **nauka, sztuka i archeologia**
- **kontrola linii energetycznych, kontrola GIS**



Badania Nieniszczące i Diagnostyka
Agenda Wydawnicza SIMP
ul. Sabaly 11a, 71-341 Szczecin
e-mail: wydawnictwo@ptbnidt.pl
www.bnid.pl

ZESPÓŁ REDAKCYJNY / EDITORIAL BOARD

REDAKTOR NACZELNY / EDITOR-IN-CHIEF
Tomasz Chady

Z-CY REDAKTORA NACZELNEGO / DEPUTES EDITOR-IN-CHIEF
Adam Sajek
Ryszard Pakos

CZŁONKOWIE REDAKCJI / MEMBERS OF THE BOARD
Jacek Grochowalski
Ryszard Łukaszk

REDAKTORZY DZIAŁOWI / SECTION EDITORS

METODOLOGIA BADAŃ / RESEARCH METHODOLOGY
Sławomir Mackiewicz, Marek Śliwowski

CERTYFIKACJA W BADANIACH / CERTIFICATION IN RESEARCH
Bogdan Piekarczyk

URZĄDZENIA I SYSTEMY BADAŃ
/ EQUIPMENT AND SYSTEMS FOR RESEARCH
Grzegorz Jezierski, Marek Lipnicki

PRAKTYKA PRZEMYSŁOWA BADAŃ
/ PRACTICE OF INDUSTRIAL RESEARCH
Krzysztof Dragan, Darek Wojdała

DIAGNOSTYKA / DIAGNOSTICS
Bogusław Ładecki,

MIĘDZYNARODOWA RADA PROGRAMOWA
INTERNATIONAL SCIENTIFIC COMMITTEE

Prof. Ryszard Sikora, *Zachodniopomorski Uniwersytet Technologiczny w Szczecinie, Przewodniczący/President*

Prof. Krishnan Balasubramaniam, *Indian Institute of Technology Madras, Chennai, India*
Prof. Alexander Balitskii, *National Academy of Science of Ukraine, Ukraine*

Prof. Gilmar F. Batalha, *University of Sao Paulo, Brasil*

Prof. Leonard J. Bond, *Iowa State University, USA*

Dr Pierre Calmon, *CEA, France*

Prof. Ermanno Cardelli, *Università degli Studi di Perugia, Italy*

Prof. Zhenmao Chen, *Xi'an Jiaotong University, China*

Prof. Leszek A. Dobrzański, *World Academy of Materials and Manufacturing Eng., Polska*

Dr Hubert Drzeniek, *AMIL Werkstofftechnologie GmbH, Germany*

Prof. Antonio Faba, *Università degli Studi di Perugia, Italy*

Prof. Nikolaos Gouskos, *University of Athens, Grece*

Mgr Paweł Grześkowiak, *UDT, Polska*

Prof. Jerzy Hoła, *Politechnika Wroclawska, Polska*

Prof. Jolanta Janczak-Rusch, *Empa, Switzerland*

Mgr Ryszard Jawor, *Ryszard Jawor Usługi NDT, Polska*

Dr Grzegorz Jezierski, *Politechnika Opolska, Polska*

Inż. Sławomir Józwiak, *NDT Systems, Polska*

Mgr Pablo Katchadjian, *National Atomic Energy Commission of Argentina, Argentina*

Mgr Jan Kielczyk, *Energomontaż-Północ, Polska*

Mgr Jacek Kozłowski, *TEST PLB, Polska*

Prof. Marc Kreutzbruck, *University of Stuttgart, Germany*

Dr. Jochen Kurz, *DB Systemtechnik GmbH, Germany*

Mgr Marek Lipnicki, *KOLI, Polska*

Prof. Leonid M. Lobanow, *Paton Welding Institute, Ukraine*

Dr Sławomir Mackiewicz, *NDT SOFT, Polska*

Dr Wojciech Manaj, *Instytut Lotnictwa, Polska*

Dr Tadeusz Morawski, *Usługi Techniczne i Ekonomiczne "Level", Polska*

Prof. Zinovy T. Nazarchuk, *National Academy of Science of Ukraine, Ukraine*

Dr Ryszard Nowicki, *GE Energy, Polska*

Prof. Mohachiro Oka, *Oita National College of Technology, Japan*

Dr Jolanta Radziszewska-Wolińska, *Instytut Kolejnictwa, Polska*

Prof. Helena Maria Geirinhas Ramos, *Instituto Superior Técnico, Portugal*

Prof. Joao M A Rebello, *Federal University of Rio de Janeiro, Brasil*

Prof. Artur Lopes Ribeiro, *Instituto Superior Técnico, Portugal*

Prof. Maria Helena Robert, *University of Campinas, Brasil*

Dr hab. Maciej Roskosz, *Politechnika Śląska, Polska*

Prof. Krzysztof Schabowicz, *Politechnika Wroclawska, Polska*

Prof. Valentin R. Skalsky, *National Academy of Science of Ukraine, Ukraine*

Prof. Jacek Stania, *Łukasiewicz – Górnos Śląski Instytut Technologiczny, Polska*

Prof. Jacek Szelażek, *IPPT PAN, Polska*

Dr Marek Śliwowski, *NDTEST Warszawa, Polska*

Prof. Antonello Tamburrino, *University of Cassino and Southern Lazio, Italia*

Prof. Yuji Tsuchida, *Oita University, Japan*

Prof. Andrzej Tytko, *AGH Kraków, Polska*

Prof. Lalita Udpa, *Michigan State University, USA*

Prof. Gábor Vértesy, *Hungarian Academy of Sciences, Hungary*

Dr Grzegorz Wojas, *UDT, Polska*

Prof. Sławomir Wronka, *Narodowe Centrum Badań Jądrowych, Polska*

Prof. Chunguang Xu, *Beijing Institute of Technology, China*

Prof. Noritaka Yusa, *Tohoku University, Japan*

Badania Nieniszczące i Diagnostyka

Nondestructive Testing and Diagnostics

NR 1-4/2023

ISSN 2451-4462 (ONLINE: 2543-7755)

VOLUMEN 8

SPIS TREŚCI

Adam Kondej, Dominik Kukla

Nieniszcząca ocena grubości przypowierzchniowej warstwy azotków w technicznych stopach żelaza metodą prądów wirowych* 12

Tomasz Katz

Modelowanie wykrywania wad kontaktowozmęczenia w szynach kolejowych metodą ultradźwiękową* 17

Piotr Bielawski

Diagnozowanie potencjału eksploatacyjnego zespołu maszyn* 25

Tomasz Gorzelańczyk, Krzysztof Schabowicz

Przegląd nowoczesnych metod nieniszczących wykorzystywanych do badania płyt włóknisto-cementowych* 30

Alireza Akhlaghi

Porosity measurement in CFRP* 37

Jerzy Kaszyński

Problematyka badań nieniszczących w budownictwie na krajowych konferencjach KKBN - przeżyjmy to jeszcze raz 40

Maciej Martyna, Roman Martyna

Możliwości i ograniczenia magnetycznej metody MRT badania stanu technicznego lin stalowych w czasie ich eksploatacji na urządzeniach dźwignicowych* 48

Mateusz Cybulski, Marek Lipnicki, Krzysztof Mroczek, Rafał Obląkowski

Badania ultradźwiękowe Phased Array złączów choinkowych stopki łopaty stopni L-0 po stronie turbiny i generatora w elektrowni jądrowej w Szwecji* 56

Bartosz Hyla, Michał Sobczak, Jakub Roemer

Badania nieniszczące materiałów kompozytowych metodą termografii laserowej* 62

Mateusz Napiórkowski, Mariusz Szóstak, Krzysztof Schabowicz

Nieniszczące, wizualne metody badań wykorzystujące wirtualną rzeczywistość w budownictwie – stan wiedzy* 67

Mateusz Wróbel, Maciej Szwed

Fitness for service dla urządzeń ciśnieniowych – doświadczenia UDT* 72

Maciej Szwed, Tomasz Jakubowski, Michał Targoński

Detekcja pęcherzy wodorowych metodami ultradźwiękowymi TOFD, TULA i Phased Array* 80

Karol Kaczmarek

Wymagania normy PN-EN ISO 9712 dla egzaminu praktycznego w sektorach przemysłowych* 88

Marcin Lewandowski, Jakub Rozbicki, Hanna Smach, Piotr Karwat,

Arkadiusz Szczurek, Jolanta Sala, Alicja Bera
Modelowe rozwiązania skanerów UTPA do badań spawów dla wież wiatrowych, sekcji płaskich oraz konstrukcji wielkogabarytowych on-shore/off-shore* 97

Jakub Spytek, Kajetan Dziedzic, Łukasz Ambroziński, Łukasz Pieczonka

Obrazowanie wad w strukturach cienkościennych z wykorzystaniem ultradźwiękowych fal przewodzonych* 101

Streszczenia artykułów zgłoszonych na 50. KKBN 105

Bogusław Ładecki, Joanna Augustyn-Nadzieja

Problemy pęknięcia zmęczeniowego wału wirnika wentylatora ze stali C45* 120

Informacje BNID - Wspomnienie o plk. dr. inż. Romanie OSTROWSKIM 124

Informacje dla Autorów i Czytelników 125

* Artykuł recenzowany

PATRONAT I STAŁA WSPÓŁPRACA
PATRONAGE AND PERMANENT COOPERATION



PTBNiDT

Alireza Akhlaghi*

Dolphitech LTD

Porosity measurement in CFRP

ABSTRACT

Single point, amplitude distributions and area measurements via Matrix Array Ultrasonic Testing (MAUT) software tools can provide users numerous options and versatility to characterise and quantify porosity. These measurement tools can specifically be beneficial in Live Mode when capturing data for better visualisation and will lead to a more accurate decision-making. Although the application examples highlighted in this presentation are mainly focused on porosity measurements, such ultrasonic workflow can be fine-tuned and adopted for many other inspection tasks as a quantitative test method. This case study is carried out by utilising the MAUT technology as a new and pioneer technique for porosity evaluation.

Keywords: MAUT, Matrix Array Ultrasonic Testing; Porosity; Disbound; Delamination

1. Introduction

Distributed microporosity is always an issue as it can weaken the material and adversely affect the mechanical properties and durability of the components. Moreover, even if the overall porosity content remains below a threshold that causes a significant reduction in mechanical performance, its presence can mask the detection of other subsurface flaws and more critical defects such as disbound and delamination.

To demonstrate the variation in detectability of porosity, CFRP panels of different porosity levels were manufactured with flat bottom holes by Flying S Inc. for inspection with the MAUT instrument, the FBH samples mimic the response from a disbound or delamination like real application example.

The CFRP panels are made from T700S plain weave carbon fibre prepreg, which is 42% epoxy resin by weight. Three panels were made, where curing was performed at three different vacuum levels (50%, 75%, and 100%). 100% vacuum represents the nominal cure cycle, with 75% and 50% vacuums used to intentionally introduce higher levels of porosity. Each panel is made to the same specifications otherwise and looks like the panel pictured in Figure 1.

When dealing with real application examples porosity can have a significant impact on measurements and the overall

characterisation of the defects, this case study was carried out with FBH samples at varies dimensions to mimic this effect as high level of porosity can make it extremely difficult to detect such discontinuation of material when utilising ultrasonic testing equipment.

Each panel has five FBH samples, which can be seen from the “back face” in figure 1. The dimensions of the FBH are shown in figure 2. The holes will be labelled using their nominal diameter and depth to the nearest millimetre in this study.

Due to variation in the detectability of defects with porosity, it is also important to identify panels with higher porosity. This study will cover both the variation in the detectability of defects with porosity and how to distinguish more porous samples accordingly.

2. Solution

The panels were inspected utilizing MAUT equipment with 2.5MHz transducer module (TRM). This TRM has a central frequency of 2.5 MHz and an Aqualene delay line. It is suited to lower-grade composite material inspection, including materials with higher porosity levels.

A stitched map consisting of 5x5 tiles was acquired over the inspection surface to perform live C-Scans inspection.

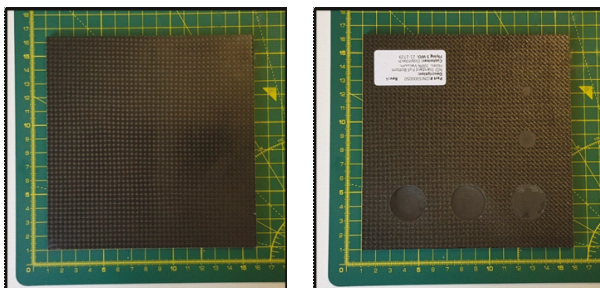


Figure 1. Photographs showing the appearance of the panels. The panel cured in a 100% vacuum is shown as an example. (a) shows the “inspection face” and (b) shows the “back face” of the panel.

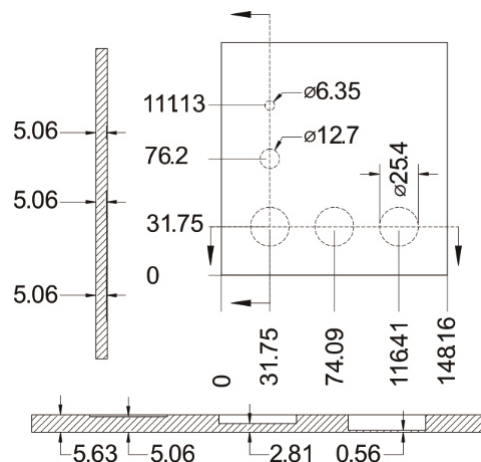


Figure 2. Technical drawing of the panel. Dimensions are given in millimetres.

*Corresponding author.

E-mail: alireza.akhlaghi@dolphitech.com

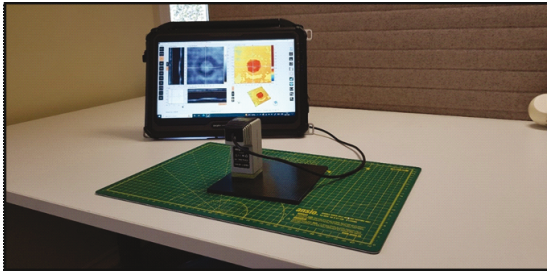


Figure 3. Photograph of setup on a panel using a MAUT and 2.5MHz TRM.

This is carried out freehand by positioning the TRM on the inspection area based on the predefined grid and stitching the data from each location together. A standard ultrasonic gel was used as the couplant.

This study will cover the variation in the detectability of defects with porosity and how to distinguish more porous samples. The MAUT instruments signal-to-reference tool will be used to quantify the difference between the desired signal and background level to show the variation in the detectability of the defects with porosity. The back wall amplitude is expected to reduce with porosity, which can be used as indication of distinguishing panels of different porosities. This is because the pores scatter the ultrasound as it travels through the material, so the level of sound energy received as an echo from the opposite surface of the material is significantly reduced.

Values used in these calculations for the signal-to-reference and back wall amplitude are taken from the average of measurements over a larger region. Using data over a large area provides a more representative measurement and, as a result, increased confidence. This is particularly advantageous for anisotropic materials such as composites where point measurements may vary significantly over small areas. MAUT software tools simplify this process by utilising live analysis tools over the 128x128 electrodes providing 16384 virtual elements.

This paper also highlights how imaging and thresholding of the data can be used to visualize areas of higher porosity, where the area covered can be another quantitative indicator of the porosity of the sample.

3. Challenges

The porosity content of the panels is higher when cured in a lower vacuum. This makes the material more attenuative and consequently, a lower frequency transducer is needed to penetrate the material. A 2.5 MHz TRM was chosen as a compromise between needing to penetrate the material and retaining the resolution needed to accurately image the defects.

4. Findings

The signal-to-reference tool was used on the manually stitched data set with the data gated to contain the relevant reflector as shown in figure 4. The area that the reference value was calculated from was kept consistent, covering an

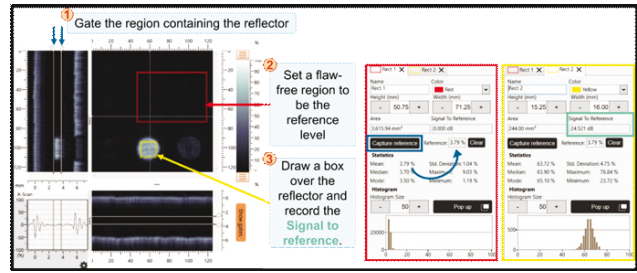


Figure 4. Process for calculating signal-to-reference for each reflector.

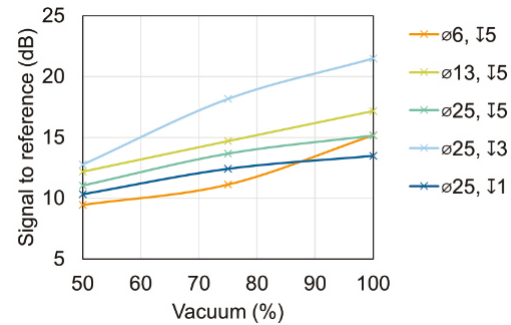


Figure 5. Signal-to-reference of reflectors. The reflectors are labelled using their nominal diameter and depth from the inspection surface to the nearest millimetre.

area slightly over 3600 mm² in size and with approximately 58,000 A-Scans. The resulting signal-to-reference values are shown in figure 5.

In figure 5, the signal-to-reference can be seen to reduce with lower vacuum levels, whereby the mean signal-to-reference for the 100% vacuum panel is 17.2 dB, compared to 14.4 dB and 11.4 dB for 75% and 50% vacuum panels respectively. The lower vacuum levels correspond to higher porosities, where the reduction in signal-to-reference is the result of porosity scattering the ultrasound, resulting in higher levels of noise and less signal from the defects themselves. It highlights the need to ensure porosity content is low to ensure defects are detected.

There are different ways of identifying panels with higher porosity. As highlighted, one method is the reduction in back wall amplitude, as panels with higher porosity are expected to be more attenuative to ultrasound. The amplitude is taken over the same area as the reference region in figure 4, but with just the back wall gated. The results are shown in figure 6.

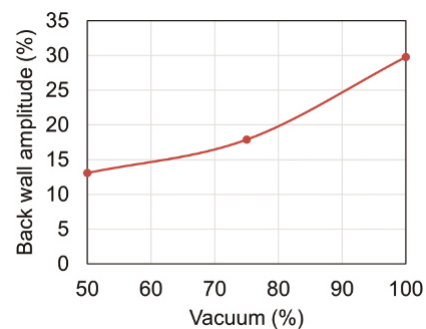


Figure 6. Back wall amplitude of panels cured in different vacuum levels.

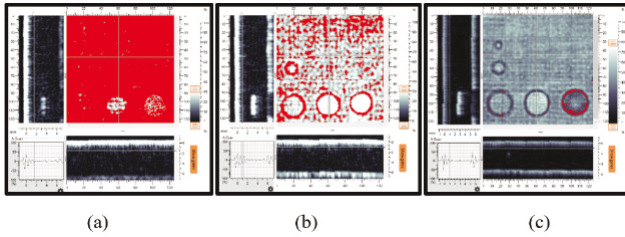


Figure 7. Amplitude view for manually stitched data on panels cured in (a) 50%, (b) 75% and (c) 100% vacuum.

In figure 6, the back wall amplitude reduces with lower vacuum and thus higher porosity. This confirms that the back wall amplitude reduces with increased porosity level. The change is significant and thus the panels of different porosity levels can clearly be distinguished.

To visualise areas of higher porosity, a threshold on amplitude of the C-Scan display can also be utilised. Figure 7 shows the result for a 20% amplitude threshold using the Defect Detection tool of the MAUT analysis tool. This is an effective approach for a quick pass/fail screening of composites, when the percentage amplitude that corresponds to an excessive level of porosity is known.

The panels are cured in a lower vacuum, to increase their porosity, have a larger area highlighted in red, which corresponds to larger areas of low amplitude. This is clearly visible in the A-Scan where a digital display threshold is used to show low amplitude areas in red to be highlighted in the C-Scans respectively to help differentiate the high and low porosity samples from each other. This also helps quantify the fractional area plotted in figure 8, useful for procedures that stipulate a maximum allowable porosity by area fraction.

There may be scenarios where defects need to be detected on more porous samples. Fortunately, the ability to detect

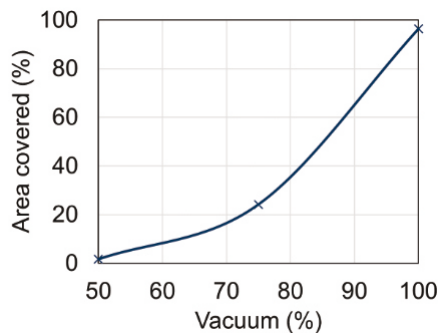


Figure 8. The area covered by the threshold region for panels cured in different vacuum levels.

the reflectors is better than what some of the signal-to-reference values may suggest. Figure 9 shows the manual stitch on the 50% vacuum panel, which represents the most porous and thus, most difficult to inspect panel. In figure 9, the thickness (ToF) view is shown with the back wall included in subfigure (a), and the ToF view is shown with internal gating and a threshold applied to help emphasize the flat bottom holes in subfigure (b).

All five of the flaws are clear to see in this thickness (ToF) view. Thus, the C-Scans reduce the problem to one of pattern

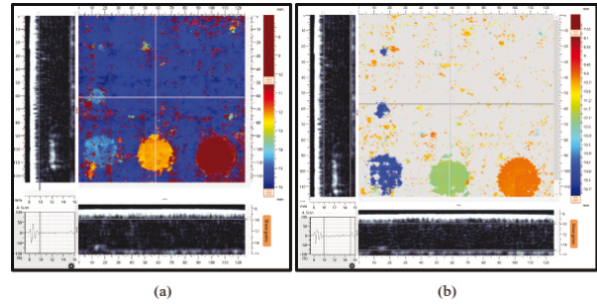


Figure 9. Thickness view of manual stitch taken on 50% vacuum panel. (a) shows the data with the back wall included, and (b) shows the data with internal gating and the amplitude threshold set to 12.5%.

recognition, which humans are well suited to, indicating that there are potentials to detect defects in more porous samples, if necessary. Hence making MAUT live C-Scans entirely unique when compared to traditional A-Scan displays.

5. Conclusion

With the live C-Scans and onboard statistical analysis, MAUT technology offers both detailed images and numerical data. The MAUT test principle is unique in providing live C-Scans from its 16384 virtual elements, and simultaneously enabling the operator to manually stitch the scanned data together for the inspection area. Allowing a rapid data acquisition and mapping.

The MAUT software tools for analysis also offer the functionality to perform statistics on board, where the defect signal strength could be quantified. This is noticeable as the signal-to-reference at the reflector depth was seen to greatly reduce with porosity.

The mean signal-to-reference for the 100% vacuum panel is 17.2 dB, compared to 14.4 dB and 11.4 dB for 75% and 50% vacuum panels respectively, whereby a lower vacuum corresponds to a higher porosity. This highlights the need to ensure porosity content is low, highlighting the “dangers” of porosity in their ability to mask other subsurface flaws and more critical defects such as disbond and delamination. If defects are to be detected and characterised in more porous samples, the MAUT live analysis software can generate C-Scans with ease, facilitating interpretation compared to conventional A-Scan displays.

To quantify the level of porosity, the average back wall amplitude can be monitored, or the Defect Detection tools can be utilised, enabling rapid Pass/Fail quality control according to a variety of required criteria.

6. Literature

This paper is based on a practical case study carried out by utilising the unique MAUT technology hence no current reference to any existing literature is available to the best knowledge of the original and subsequent authors. The measurements were carried out in line with the ASTM E3370-22 (Standard Practice for Matrix Array Ultrasonic Testing of Composites, Sandwich Core Constructions, and Metals Used in Aerospace Applications).